Research Article

Van Khiem Nguyen, Duy Khanh Pham, Ngoc Quyen Tran, Le Hang Dang, Ngoc Hoa Nguyen, Thanh Mien Nguyen, Nguyen Thanh Viet, Jin-Woo Oh, Thi-Diem Bui, and Bich Thi Luong*

Effect of stabilizers on Mn ZnSe quantum dots synthesized by using green method

https://doi.org/10.1515/gps-2022-0032
received November 16, 2021; accepted February 03, 2022

Abstract: Herein, the effect of three types of capping polymers, mercaptopropionic acid (MPA), polyethylene glycol (PEG), and starch on the photoluminescence of Mn(2+)-doped ZnSe (ZnSe:Mn) nanoparticles, has been investigated. ZnSe:Mn nanoparticles were successfully prepared with a green method of precipitation in aqueous solutions containing MPA, PEG, or starch as stabilizers. The X-ray photoelectron spectroscopy and Fourier-transform infrared spectroscopy had proved the formation of ZnSe:Mn particles and the interaction between them and the capping agents. The resultant nanoparticles with different capping polymers were identical in optical property; however, photoluminescence quantum yields (PLQY) as well as the photoluminescence lifetime varied by capping agents. Starch-capped ZnSe:Mn nanoparticles had the biggest size compared to others, which was confirmed using transmission electron microscopy, dynamic light scattering, UV-Vis absorbance and Raman spectroscopy. Also, the PL intensity was significantly enhanced with starch-capped ZnSe:Mn nanoparticles. The PLQYs of starch archived 26%, which was 1.23 or 1.8 times lower than that of ZnSe:Mn nanoparticles capping with MPA or PEG, respectively. Furthermore, the highest decline of PL intensity was detected in PEG, which completely diminished in the 19th week, while both MPA and starch endowed ZnSe:Mn nanoparticles with outstanding PL lifetimes diminished over seven weeks.

Keywords: luminescent nanoparticles, green synthesis, capping agents

*** Corresponding author: Bich Thi Luong,** Institute of Applied Materials Science, Viet Nam Academy of Science and Technology, Ho Chi Minh City 70000, Vietnam; Graduate University of Science and Technology, Vietnam Academy of Science and Technology, Ha Noi City 100000, Vietnam, e-mail: luongthibich@iams.vast.vn
Van Khiem Nguyen: Institute of Applied Materials Science, Viet Nam Academy of Science and Technology, Ho Chi Minh City 70000, Vietnam; Department of Tissue Engineering and Regenerative Medicine, School of Biomedical Engineering, International University, Vietnam National University-Ho Chi Minh City (VNU-HCM), 700000, Vietnam
Duy Khanh Pham, Ngoc Quyen Tran, Le Hang Dang: Institute of Applied Materials Science, Viet Nam Academy of Science and Technology, Ho Chi Minh City 70000, Vietnam; Graduate University of Science and Technology, Vietnam Academy of Science and Technology, Ha Noi City 100000, Vietnam
Ngoc Hoa Nguyen: Faculty of Chemical Engineering, HCMC University of Food Industry, Ho Chi Minh City 700000, Vietnam
Thanh Mien Nguyen, Jin-Woo Oh: Department of Nano Fusion Technology, Pusan National University, Busan 46214, Republic of Korea
Nguyen Thanh Viet: Institute of Environmental Technology and Sustainable Development, Nguyen Tat Thanh University, Ho Chi Minh City 72800, Vietnam
Thi-Diem Bui: Graduate University of Science and Technology, Vietnam Academy of Science and Technology, Ha Noi City 100000, Vietnam; Faculty of Chemical Engineering, Industrial University of Ho Chi Minh City, Ho Chi Minh City 700000, Vietnam

1 Introduction

Colloidal semiconductor nanomaterials have gained concerns recently because of their unusual electrical and optical characteristics. Interestingly, inorganic lumiphores with high quantum efficiencies, color-tunable, and narrow emission spectra, and exceptional chemical stability are direct bandgap semiconductor nanocrystals [1–3]. Nowadays, nanocrystals have several applications in light-emitting diodes (LEDs), lasers, biological and chemical sensors, and solar cells due to these features [1,4–6]. Due to their intense emission of dopants, doping with atomic impurities is an efficient technique to make luminous nanocrystals [7–9]. In order for the dopant to rapidly absorb the excitation energy for generating luminescent of the dopant, the excitation energy of the dopant needs to be smaller than the bandgap of host materials. Ag dopant atoms could be used as an optical filter for polychromatic light of nanosized Mn:ZnSe quantum dots (QDs) to improve the monochromaticity of the light. ZnSe bandgap and trap emissions can be filtered out after Ag doping in QDs, leaving only Mn dopant

Open Access. © 2022 Van Khiem Nguyen *et al.*, published by De Gruyter. This work is licensed under the Creative Commons Attribution 4.0 International License.

emission with increased monochromaticity. It is confirmed that Ag doping will provide a new quicker deactivation mechanism from the ZnSe conduction band to the Ag energy level, resulting in fewer electrons being deactivated via ZnSe bandgap emission and ZnSe trap emission. As a result, Mn dopant emission is the only one left [10]. Moreover, ZnSe is a potential semiconductor with a bandgap of 2.7 eV at an ambient temperature and a transmittance range of 0.5–22 m. Researchers synthesized high-quality ZnSe nanocrystals using organometallic methods, which is uneconomic and environmentally unfriendly [11–13]. Recently, Murase and Gao synthesized blue-emitting ZnSe nanocrystals in an aqueous solution; however, their properties are highly toxic and they have oxidative H_2Se gas as the selenium precursor source [14]. This synthetic technique is to not only develop environmentally friendly but also sustainable methods for the synthesis of nanoparticles, which use nontoxic chemicals, environmental solvents, and renewable materials to evade adverse effects in medical applications [15].

To preserve the structural properties of synthesized nanoparticles, many capping agents such as thiophenol, thiourea, and mercaptoacetate have been studied for semiconductors synthesis [16–18]. However, these are toxic and harmful to the environment, thus the green method should be developed [19–22]. The imidazole Mn:ZnS-capped QD, with its water solubility and strong connectivity with the biological world as well as their rings containing nitrogen as hetero-atoms, will have the potential to be used in bio-mimicking materials where the enzymes like carbonic anhydrase can be mimicked using zinc as the metal ion and imidazole as a ligand [23]. Furthermore, by using different amines as coordinating ligands, the shape of these doped ZnSe:Mn^{2+} and CdS:Mn^{2+} semiconductor nanocrystals can be easily controlled via a single-step synthetic method. It is found that there exists the threshold for doping concentration of maximum photoluminescence (PL) intensity and this value for 1D nanorods is smaller than that of 0D QDs. The PL intensity of the doped nanocrystals can be further enhanced by passivating them with ZnS or ZnSe outer shells [13].

Nevertheless, II–VI semiconductor nanoparticles are themselves highly unstable agglomerate or they can coalesce extremely quickly due to the absence of a trapping medium or some other forms of encapsulation or uncontrolled growth of particles [24,25]. Moreover, the optoelectronic properties of nanoparticles are significantly influenced by the surface passivation and the surface state, which are provided and improved via the bonding of capping agents to the nanoparticles [26,27]. In general, the agglomeration of nanoparticles can be prevented by electrostatic stabilization and steric hindrances. In the solution, when a polymer is adsorbed onto a surface of nanoparticles, it generally does not lie flat. Thus, a polymer can provide a strong repulsion between two approaching surfaces due to two such polymer layers overlapping at a collision distance between the particles. A small portion of the molecule must be tightly adsorbed to the underlying nanoparticle surface while most of the polymer chain should extend from the surface since the particles are isolated [28]. Therefore, the ZnS–Mn^{2+} samples were prepared by a chemical precipitation method using nonionic surfactants as capping agents such as polyethylene glycol (PEG) and poly (amino amide) [29]. The simple synthesis of the ZnS nanoparticles capped with green capping molecules such as polyvinyl pyrrolidone and PEG by homogeneous precipitation technique, and the preparation of the polymer nanocomposite have been reported. The PEG-capped ZnS nanoparticles were allowed to react with poly-DADMAC to form the polymer nanocomposites [30]. Besides, Stabilizers were substances used in nanotechnology to create and maintain the nano shape and size of the particles, and they help nanoparticles enhance their volume as well as surface area [31–33]. The types of nanoparticles and the process of synthesis affect the choice of the stabilizers. Surface change with stabilizers is important for preventing the adhesion of particles and obtaining a firm particle suspension [33]. First, starch is a substance formed from anhydro-glucose systems forming a couple of main polymers, particularly amylopectin and amylose [34]. Furthermore, some studies have explained that this kind of polysaccharide contains the function for biomedical purposes, such as substrates for cell spreading [35], structures for tissue design [36–39], drug delivery methods [40–45], and implants [46]. Second, PEG is a polymer containing unique properties such as hydrophilic, low toxicity, and biocompatible that can be applied for medical applications [47]. Hence, this type of polymer was widely acceptable for biomedical applications. Finally, mercaptopropionic acid (MPA) is usually chosen to serve as a capping ligand in the preparation of ZnSe or other II–IV semiconductor nanocrystals (NCs) by the aqueous route, due to its preferable binding capacity. One molecule of MPA can coordinate to one metal atom site to form the most favorable hexagonal configuration; thus, enhancing the colloidal stability of the formed NCs which is favorable for PL performance. Moreover, the hydrophilic carboxylic

groups at the outer surface render excellent water solubility for NCs after the thiol group has bonded to the zinc and manganese ions on their surfaces [2].

Therefore, in this study, there were three stabilizers, including starch, PEG, and MPA chosen to synthesize ZnSe:Mn NPs and enhance luminescence intensity as well as biocompatibility of these nanoparticles for wide biomedicine application.

In this study, we reported the synthesis of low-toxicity ZnSe:Mn nanocrystals with manganese resulting in visible phosphorescence from the Mn^{2+} with 4T1 → 6A1 transition centered at 580 nm. Moreover, the ZnSe:Mn were synthesized in the aqueous phase using various capping agents such as starch, PEG, and MPA as a stabilizer at low temperatures (80–100°C). This synthetic process is green due to the use of water as a solvent. It is seen that the effect of stabilizing agents on the crystal structure and the nanoparticle size led to affecting the morphology and optical properties of ZnSe:Mn QDs.

2 Materials and methods

2.1 Materials

Manganese(II) acetate (Mn $(CH_3COO)_2{\cdot}4H_2O$ 99.99%), zinc acetate ($Zn(CH_3COO)_2{\cdot}2H_2O$, 99.99%), 2-propanol (HPLC grade), 3-MPA (99 +%), sodium borohydride ($NaBH_4$, 96%), selenium powder (99.5%), polyethylene glycol (PEG 1500), and starch. All the chemicals are of analytical grade and purchased from Sigma-Aldrich.

2.2 Characterization

The photoluminescence quantum yield (PLQY) of nanocrystals was measured according to the method described in Crosby and Demas [2,3]. X-ray diffraction measurements were performed on a D/Maxrint 2000 powder X-ray diffractometer with Cu Kα radiation (λ = 1.5418 Å). The samples used for X-ray diffraction (XRD) and transmission electron microscopes (TEM) were acquired using a JEM 2100F transmission microscope with an acceleration voltage of 200 kV. The X-ray photoelectron spectroscopy (XPS) spectrum was recorded using AXIS SUPRA model with the thermos scientific Al Kα (1486.6 eV) as the X-ray source.

2.3 Method

The Zn^{2+} precursor solution was prepared following literature method [2] by dissolution of 10 mL of zinc acetate 0.1 M in 90 mL of DI water, and 40 mL of capping agents (starch, PEG, MPA) 0.1 M in three-neck flask, then the pH of this system was adjusted to pH = 6.5 using NaOH 2 M with vigorous stirring. This three-neck flask was degassed by N_2 bubble in 30 min, and the NaHSe solution was injected into the Zn^{2+} precursor solution at room temperature. The mixture was further stirred to 80–100°C relating to the capping agent and refluxed for 3 h for complete ZnSe:Mn crystals growth and age for 24 h followed by filtration. The precipitate was washed several times and dried at room temperature to give a material which readily disperses in water.

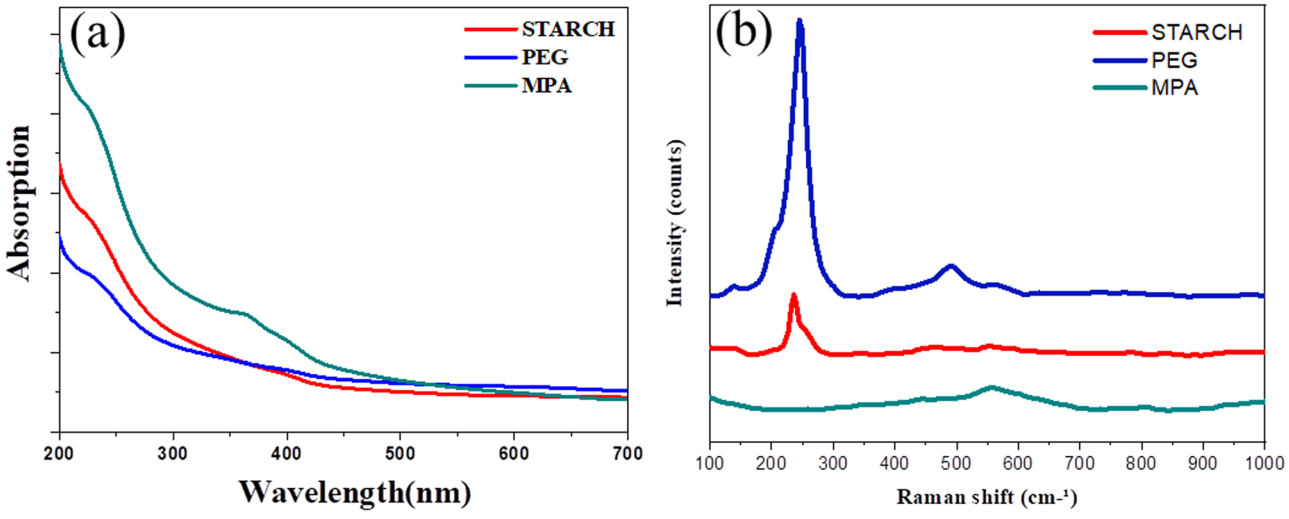

Figure 1: UV-Vis absorbance (a) and (b) Raman spectra of ZnSe:Mn using various capping agents.

3 Results and discussion

Figure 1a shows the absorptions of the nanocrystals capping with different agents. All the resultant nanoparticles display the absorptions at 230 nm corresponding to the functional organic chains of polymer or organic group, and at 350–360 nm corresponding to the band gap of ZnSe crystal. The size of the nanocrystals is totally affected by capping agents. The MPA-capped and the PEG-capped ZnSe:Mn have the absorptions at 352 nm which give the smaller size of particles [2,3].

Figure 1b shows the difference of Raman spectra relating to the difference of capping agents. The ZnSe:Mn caped MPA has one peak at 550 cm^{-1} and the ZnSe:Mn-capped starch also has one peak at 245 cm^{-1}, which means the low particles size dispersion and the size of MPA-capped nanoparticles is larger than those of ZnSe:Mn nanoparticles capped with starch and PEG. The Raman spectra shows that the size dispersion of the ZnSe:Mn PEG-capped nanoparticles is higher than those of MPA-capped or starch-capped due to two peaks at 245 and 495 cm^{-1} [48–51].

Figure 2a shows that the obtained ZnSe:Mn nanoparticles capped with different agents give light blue-emission at 420–440 nm of ZnSe band gap [52,53]. Moreover, the PL enhancement may be due to the complete removal of surface defects by passivation of the capping agent. The orange emission at 580 nm was more intense than the blue (violet) emission at 420–450 nm. This suggested that the non-radiative relaxation to the 4T1 level of Mn^{2+} is faster than the hole capture and recombination with electrons by defect states of ZnSe. Comparing the MPA, Starch- and PEG-capped ZnSe–Mn^{2+} nanoparticles, the intensity of PEG-capped PL emission was higher, indicating the increasing growth rate. The luminescent intensities were significantly increased from ZnSe:Mn capped with PEG, MPA, and starch, respectively [28]. Among these agents, starch makes the best scaffold where the

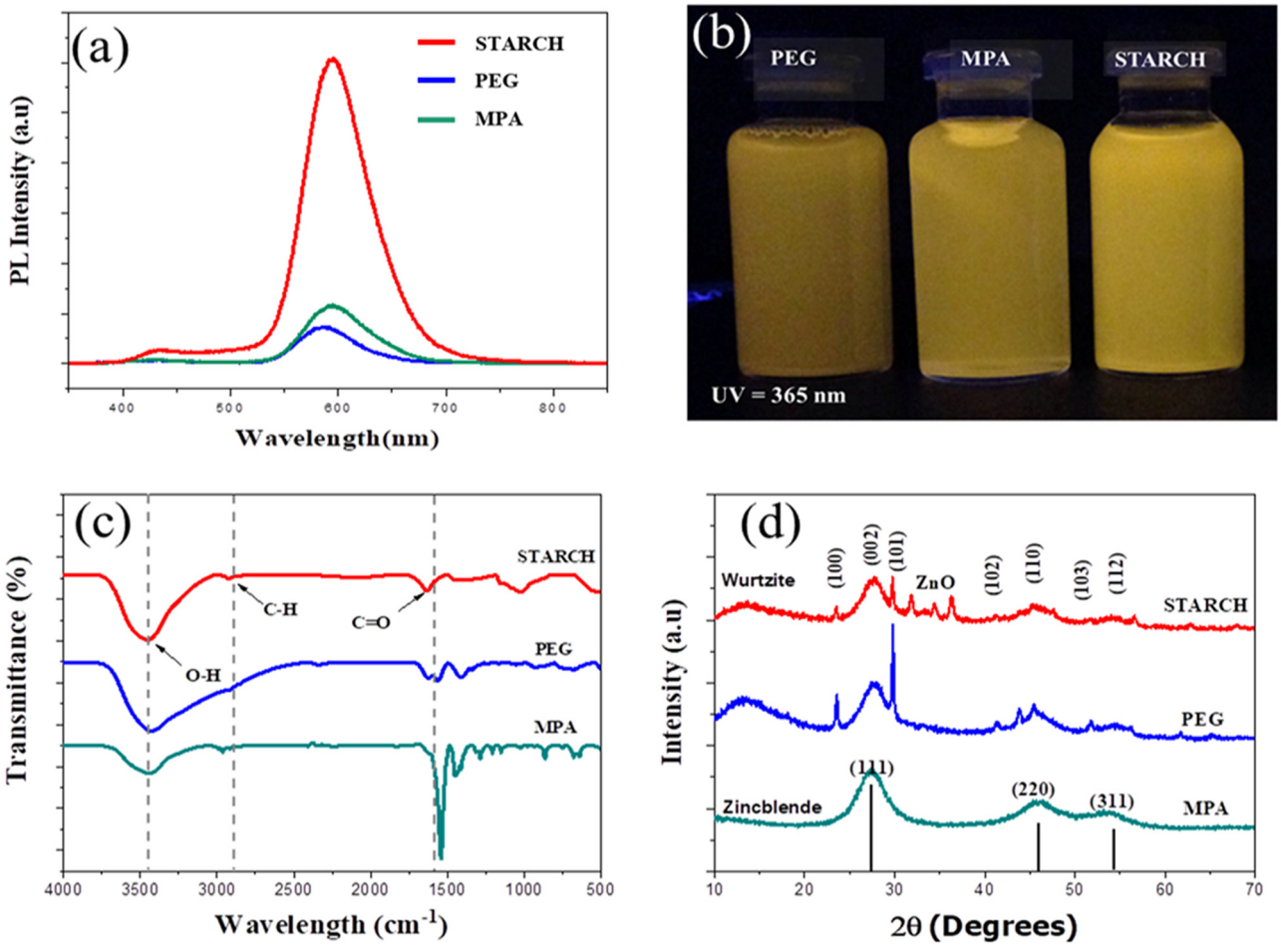

Figure 2: The characteristics of ZnSe:Mn (5%) with various capping agents, (a) PL spectra, (b) photographs of ZnSe:Mn solution were irradiated by UV (365 nm), (c) FTIR spectra, and (d) XRD patterns.

Mn^{2+} ions were absorbed inside the ZnSe crystal [54–56]. Therefore, the luminescent intensity of starch-capped ZnSe:Mn give the highest strength in the PL spectra. The color of all ZnSe:Mn solutions under UV (Figure 2b) also supports this assumption.

Fourier-transform infrared spectroscopy (FTIR) spectra were measured at ZnSe:Mn 5% doped structure to confirm the capping of the particles by capping agents shown in Figure 2c. We can observe that all samples were capped with organic compounds. The broad absorption peaks in the range 3,410–3,465 cm^{-1} corresponding to the –OH group indicates the existence of water absorbed onto the surfaces of the nanocrystals, which can be attributed to the adsorption of atmospheric water during the FTIR measurements. The band at 2,921 cm^{-1} was ascribed to the asymmetric stretching of C–H while the band at 2,370 cm^{-1} was due to the C═O, and at the one 1,500–1,650 cm^{-1} was attributed the C═O stretching mode arising from the absorption of atmospheric CO_2 onto the surfaces of the nanoparticles [20,57]. The peaks at 1,512, 1,332, and 1,340 cm^{-1} denote the formation of PEG on the surface of the ZnSe–Mn^{2+} nanoparticles [58]. This indicated that the hydrogen band was formed in the ZnSe–Mn^{2+}–PEG interface [59]. Figure 2d shows the diffraction patterns of ZnSe:Mn 5% synthesized in MPA capping agent possess zinc-blende crystal structure displayed the cubic crystals at the (111), (220), and (311) planes. PEG-capped and starch-capped ZnSe:Mn 5% have Wurtzite crystals, the XRD patterns at the (100), (101), (103), (110), and (200) planes. This supports the longer polymer chains that ZnSe:Mn can be more easily incorporated in Wurtzite (hexagonal) ZnSe Nanocrystals in cubic crystals [3,6].

The XPS in Figure 3a shows the characteristic peaks of Zn, Mn, and Se at all samples. The XPS peak at 1,017 and 1,040.4 eV in Zn 2p region correspond to the Zn $2p_{3/2}$ and Zn $2p_{1/2}$, respectively. Moreover, the binding energy values of Mn^{2+} at 652 and 659 eV imply the Mn $2p_{3/2}$ and Mn $2p_{1/2}$. The results prove that the doping Mn^{2+} into the ZnSe nanocrystal to enhance the luminescent performance is completely reasonable. On the other hand, the binding energy of Zn-2p, Mn-2p, and Se-3d between other capping agents are almost the same which provide further evidence about the uniformity in the nanocrystal [60–64].

Figure 4 shows the TEM image and particle size distribution of the various capped ZnSe:Mn nanoparticles. The TEM images indicate the monodispersed spherical crystallite. Because of swelling in the water of capping agents such as starch, PEG, the space of crystalline development was limited. Therefore, the sizes of nanoparticles are small in the range from 10 to 20 nm in Figure 4a and b. The molecular structure of PEG included polyether chains and starch also has many chains including O–H binding, they can form intermolecular hydrogen bonds

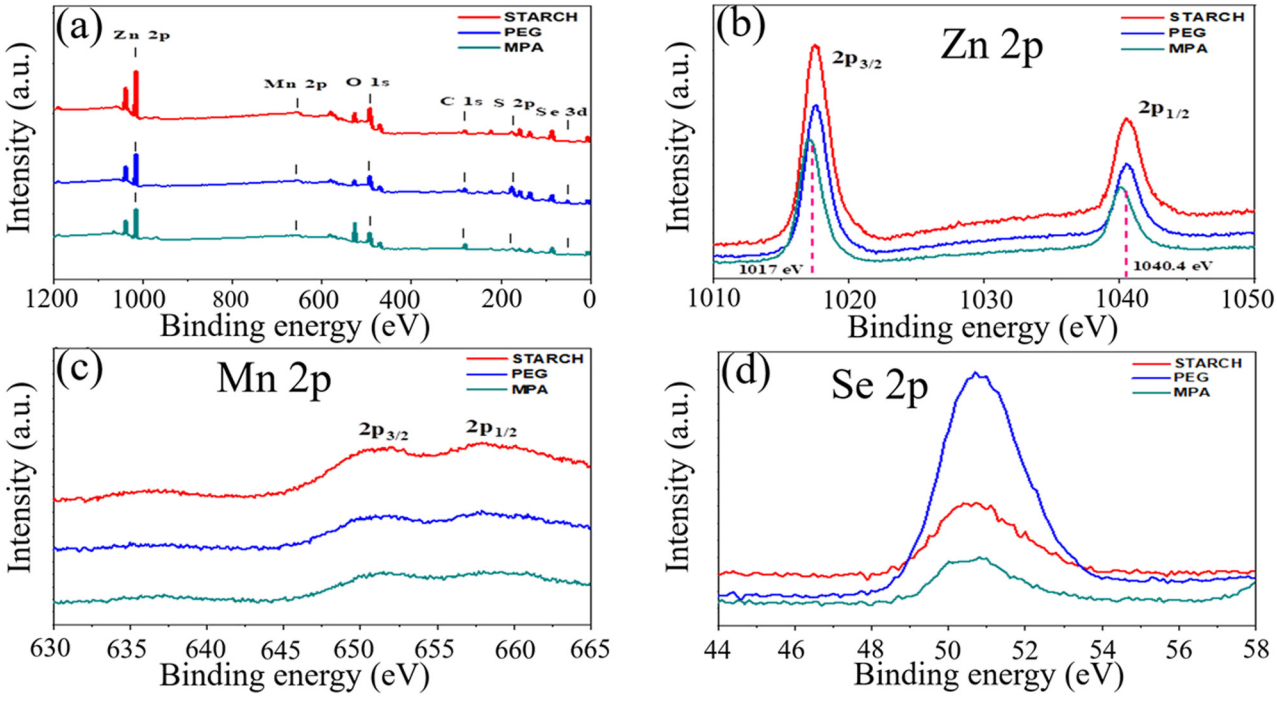

Figure 3: The XPS spectra of ZnSe:Mn (5%) at various capping agents.

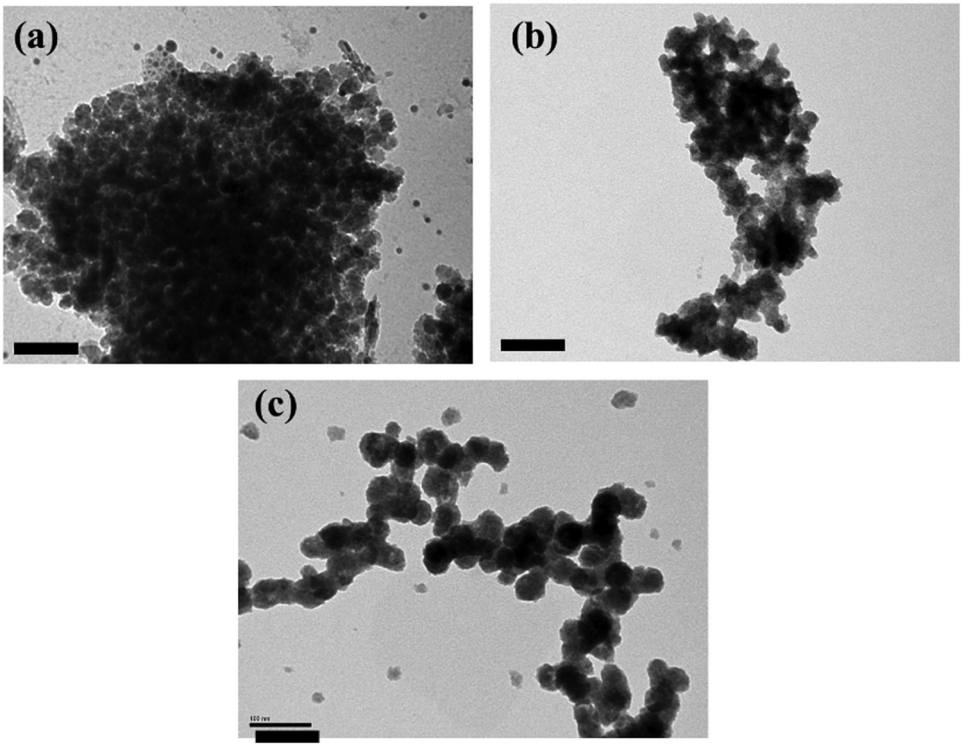

Figure 4: The TEM images of ZnSe:Mn (5%) capped with Starch (a), PEG (b), and MPA (c). Scale bar: 100 nm.

to make the scaffolds so that the nanocrystals could be produced mildly [65]. In contrast, the MPA-capped ZnSe:Mn nanoparticles have bigger spheres with 25–30 nm in diameter shown Figure 4c. It could be assessed that the side chains of the polymer as a stabilizer causes the number of doped emission ions (Mn^{2+}) and the size of nanocrystals [3,7–9]. The importance of doping Mn in ZnSe using different capping agents is that the spacing effect of agents could not influence the optical property of produced nanoparticles, but the size of capping agents and the amount of Mn^{2+} ions in ZnSe crystals are influenced.

The EDX spectrum of the ZnSe:5% Mn capped with MPA, PEG, and starch samples shown in Figure 5 indicates that the main components of the synthesized ZnSe:Mn sample are Zn and Se elements. The existence of Mn element in the product has also been found to be approximately 5%, indicating that Mn successfully integrated into ZnSe structure. In addition, the EDX peaks of C and O elements also appeared, confirming that the various stabilizers such as MPA, PEG, and starch were attached to the surface of luminescent QDs.

Figure 6 shows the PLQYs are different using rhodamine B as a photoluminescence reference. PLQY of ZnSe:5% Mn-starch capped is 26.0% (Figure 6a). The PLQY of ZnSe:Mn-starch nanoparticles is lower than those of ZnSe:Mn-MPA (32.0%, Figure 6b) and ZnSe:Mn-PEG (45.5%, Figure 6c) nanoparticles. It is caused by the structure of various capping agents. The starch structure is branched and straight chains which have a strong spacing effect and hindrance compared to MPA small molecule and PEG straight long chains [26–28].

Figure 7 displays the PL lifetime of ZnSe:Mn with various capping agents. The highest PL decay rate is detected with PEG capping. PL intensity reduced 50% after three weeks and quenched at the seventh week. Using starch as capping agents, PL intensity was diminished 50% at 6th week; however, its intensity was similar as ZnSe:Mn using PEG capping agent. Although the PL intensity of capped PEG solution is the lowest, the decay rate is very small as compared to others. After eight weeks, the quenching efficiency is around 40%, suggesting the highest stability of MPA-capped ZnSe:Mn. It was noticed that the lifetime of quantum nanoparticles is depended on the size of the nanoparticles. In this study, the hydrodynamic size of the obtained nanoparticles was around 75 nm for ZnSe:Mn-Starch, 43 nm for ZnSe:Mn-MPA, and 70 nm for ZnSe:Mn-PEG. This is explained that the PL stability depends on the spacing effect of capping agents such as their length and hindrance.

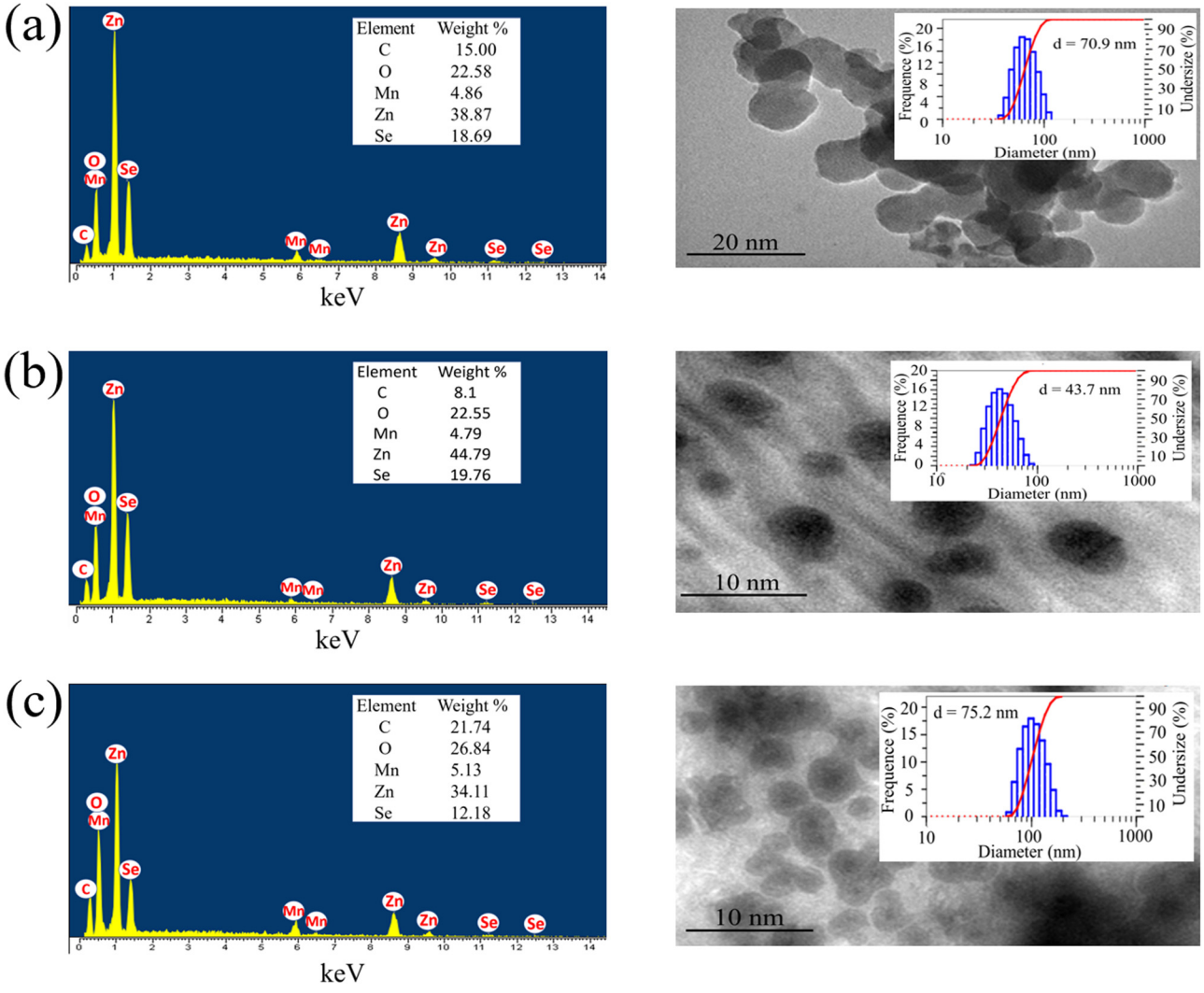

Figure 5: The EDX spectrum of the ZnSe:5% Mn capped with MPA, PEG, and starch samples.

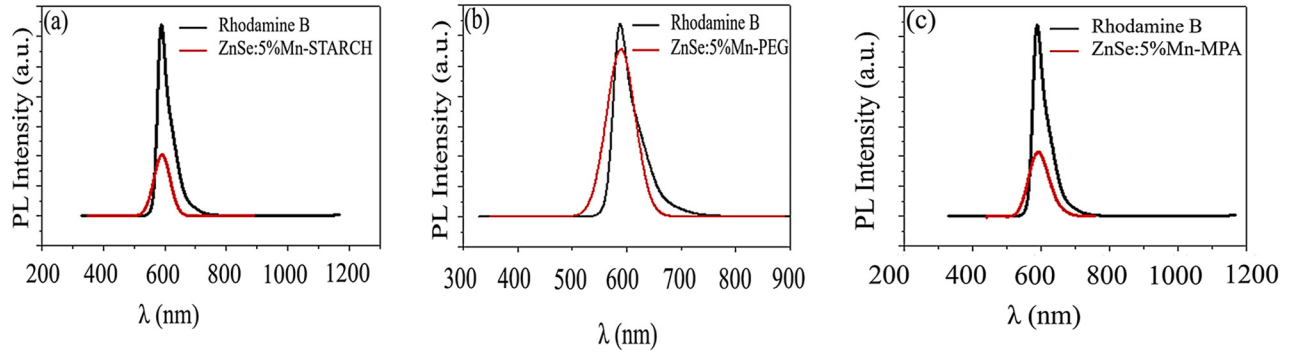

Figure 6: The PLQY compared to reference photoluminescence of ZnSe:5% Mn capped with MPA, PEG, and starch samples.

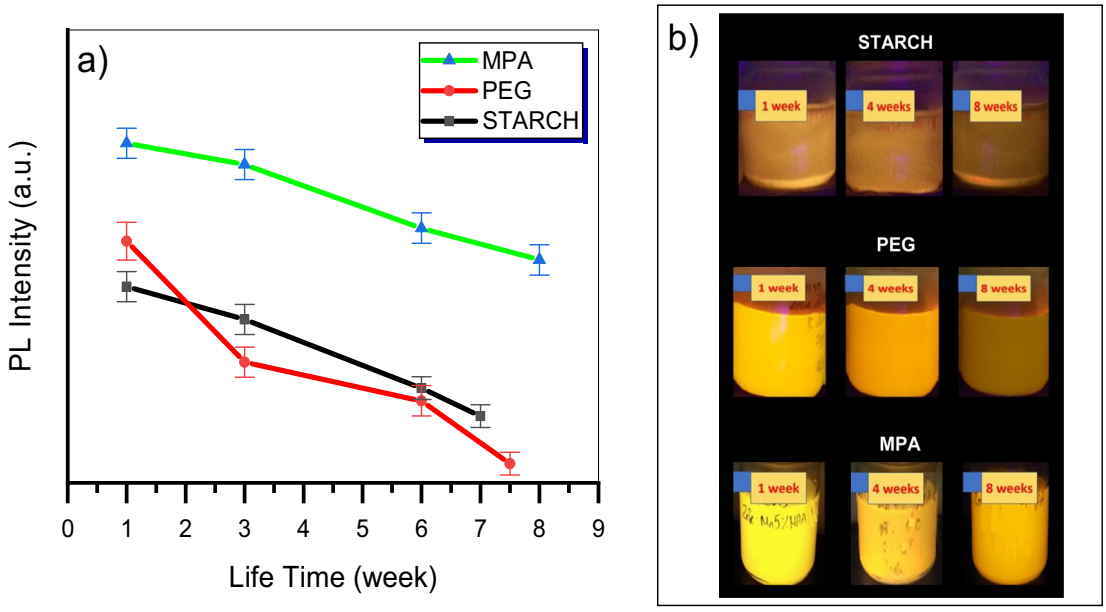

Figure 7: The PL life time of ZnSe:5%Mn capped with MPA, PEG, and starch.

4 Conclusions

A facile and environmentally friendly aqueous ZnSe:Mn nanoparticles synthesized using different capping agents, starch, PEG, and MPA were prepared in this study. All resultant ZnSe:Mn nanoparticles were well dispersed in water and had a nano-sized structure. Regarding FTIR and Raman spectra, the formation of the ZnSe:Mn nanoparticles with each capping agent, ZnSe:Mn-Starch, ZnSe:Mn-MPA, and ZnSe:Mn-PEG, have been proven. In addition, all capping structures of ZnSe:Mn nanoparticles expose orange photoluminescence bands centered at around 580 nm. However, photoluminescent features of ZnSe:Mn nanoparticles were varied due to the selection of capping agents. The PL intensity revealed the improvement of emission by changing capping agents, from PEG to MPA to starch. However, PLQY was in the following order: ZnSe:Mn-Starch (26%), ZnSe:Mn-MPA (32%), and ZnSe:Mn-PEG (45%). More importantly, the ZnSe:Mn solution capping with starch or MPA sample shows a prolonged PL lifetime, over seven weeks, while the PL intensity of PEG-capped ZnSe:Mn nanoparticles was completely diminished after seven weeks. With low cost and high sensitivity, the prepared ZnSe:Mn nanoparticles with starch as a capping agent activated in the solution during the synthesized process show promising application for LEDs, sensors, and bacteria detectors.

Acknowledgments: This work was supported by Vietnam National Foundation for Science and Technology Development (NAFOSTED). We also thank the Vietnam Academy of Science and Technology (VAST) for providing the necessary help during this work.

Funding information: This work was funded by Vietnam National Foundation for Science and Technology Development (NAFOSTED) under grant number 104.01-2017.64.

Author contributions: Bich Thi Luong: conceptualization, writing – original draft, writing – review and editing, methodology, project administration; Van Khiem Nguyen: data curation, writing – original draft, formal analysis, visualization; Duy Khanh Pham: data curation, writing – original draft, formal analysis, visualization; Thi Diem Bui: writing – original draft, data curation, formal analysis; Ngoc Quyen Tran: conceptualization, writing – review and editing, formal analysis; Le Hang Dang: writing – review and editing, formal analysis; Ngoc Hoa Nguyen: writing – review and editing, formal analysis; Thanh Mien Nguyen: writing – review and editing, formal analysis; Nguyen Thanh Viet: writing – review and editing, formal analysis; Jin-Woo Oh: writing – review and editing, formal analysis. All authors discussed the results and contributed to the final manuscript.

Conflict of interest: Authors state no conflict of interest.

Data availability statement: All data generated or analyzed during this study are included in this published article.

References

[1] Karakoti AS, Shukla R, Shanker R, Singh S. Surface functionalization of quantum dots for biological applications. Adv Colloid Interface Sci. 2015;215:28–45. doi: 10.1016/j.cis.2014.11.004.

[2] Luong BT, Hyeong E, Ji S, Kim N. Green synthesis of highly UV-orange emitting ZnSe/ZnS: Mn/ZnS core/shell/shell nanocrystals by a three-step single flask method. Rsc Adv. 2012;2(32):12132–35. doi: 10.1039/C2RA21309E.

[3] Luong BT, Hyeong E, Yoon S, Choi J, Kim N. Facile synthesis of UV-white light emission ZnSe/ZnS: Mn core/(doped) shell nanocrystals in aqueous phase. Rsc Adv. 2013;3(45):23395–23401. doi: 10.1039/C3RA44154G.

[4] Draaisma GJJ, Reardon D, Schenning APHJ, Meskers SCJ, Bastiaansen CWM. Ligand exchange as a tool to improve quantum dot miscibility in polymer composite layers used as luminescent down-shifting layers for photovoltaic applications. J Mater Chem C. 2016;4(24):5747–54. doi: 10.1039/C6TC01261B.

[5] Xiong S, Huang S, Tang A, Teng F. Synthesis and luminescence properties of water-dispersible ZnSe nanocrystals. Mater Lett. 2007;61(29):5091–4. doi: 10.1016/j.matlet.2007.04.014.

[6] Mai XT, Bui DT, Bui TT, Luong BT. Study of single-step synthesis of hyperbranced highly luminescence doped Znse:Mn, Znse:Mn/Zns quantum dots and their interactions with acid amine. J Eng Res. 2018;7:27–32.

[7] Aboulaich A, Geszke M, Balan L, Ghanbaja J, Medjahdi G, Schneider R. Water-based route to colloidal Mn-doped ZnSe and core/shell ZnSe/ZnS quantum dots. Inorg Chem. 2010;49(23):10940–8. doi: 10.1021/ic101302q.

[8] Diaz-Diestra D, Beltran-Huarac J, Bracho-Rincon DP, González-Feliciano JA, González CI, Weiner BR, et al. Biocompatible ZnS:Mn quantum dots for reactive oxygen generation and detection in aqueous media. J Nanopart Res. 2015;17(12):461–73. doi: 10.1007/s11051-015-3269-x.

[9] Parani S, Tsolekile N, May BMM, Pandian K, Oluwafemi OS. Mn-doped ZnSe quantum dots as fluorimetric mercury sensor. Nonmagnetic and magnetic quantum dots. IntechOpen; 2018. https://sci-hub.se/10.5772/intechopen.70669.

[10] Hu Z, Xu S, Xu X, Wang Z, Wang Z, Wang C, et al. Co-doping of Ag into Mn:ZnSe quantum dots: giving optical filtering effect with improved monochromaticity. Sci Rep-UK. 2015;5(1):14817. doi: 10.1038/srep14817.

[11] Gao M, Kirstein S, Möhwald H, Rogach AL, Kornowski A, Eychmüller A, et al. Strongly photoluminescent CdTe nanocrystals by proper surface modification. J Phys Chem B. 1998;102(43):8360–3. doi: 10.1021/jp9823603.

[12] Wu YA, Warner JH. Shape and property control of Mn doped ZnSe quantum dots: from branched to spherical. J Mater Chem. 2012;22(2):417–24. doi: 10.1039/C1JM14859A.

[13] Yu JH, Kim J, Hyeon T, Yang J. Facile synthesis of manganese (II)-doped ZnSe nanocrystals with controlled dimensionality. J Chem Phys. 2019;151(24):244701. doi: 10.1063/1.5128511.

[14] Murase N, Gao M. Preparation and photoluminescence of water-dispersible ZnSe nanocrystals. Mater Lett. 2004;58(30):3898–902. doi: 10.1016/j.matlet.2004.03.055.

[15] Sharma RK, Gulati S, Mehta S. Preparation of gold nanoparticles using tea: a green chemistry experiment. J Chem Educ. 2012;89(10):1316–8. doi: 10.1021/ed2002175.

[16] Choi MG, Cho MJ, Ryu H, Hong J, Chang S-K. Fluorescence signaling of thiophenol by hydrolysis of dinitrobenzenesulfonamide of 2-(2-aminophenyl) benzothiazole. Dye Pigment. 2017;143:123–8.

[17] Operamolla A, Punzi A, Farinola GM. Synthetic routes to thiol-functionalized organic semiconductors for molecular and organic electronics. Asian J Org Chem. 2017;6(2):120–38. doi: 10.1002/ajoc.201600460.

[18] Nejo AO. Synthesis of organically capped and water soluble metal sulfide semiconductor nanoparticles. University of Zululand; 2013. http://uzspace.unizulu.ac.za/bitstream/handle/10530/1320/SYNTHESIS%20OF%20ORGANICALLY%20CAPPED%20AND%20WATER%20SOLUBLE%20METAL.pdf?sequence=1&isAllowed=y.

[19] Dahl JA, Maddux BLS, Hutchison JE. Toward greener nanosynthesis. Chem Rev. 2007;107(6):2228–69. doi: 10.1021/cr050943k.

[20] Wei Q, Kang S-Z, Mu J. "Green" synthesis of starch capped CdS nanoparticles. Colloid Surf A. 2004;247(1):125–7. doi: 10.1016/j.colsurfa.2004.08.033.

[21] Murphy CJ. Sustainability as an emerging design criterion in nanoparticle synthesis and applications. J Mater Chem. 2008;18(19):2173–6. doi: 10.1039/B717456J.

[22] Senthilkumar K, Thirunavukarasu K, Samikannu K, Balasubramanin V. Low temperature method for synthesis of starch-capped ZnSe nanoparticles and its characterization studies. J Appl Phys. 2012;112:114331–53111. doi: 10.1063/1.4767924.

[23] Pandey V, Tripathi VK, Singh KK, Bhatia T, Upadhyay NK, Goyal B, et al. Nitrogen donor ligand for capping ZnS quantum dots: a quantum chemical and toxicological insight. Rsc Adv. 2019;9(49):28510–24. doi: 10.1039/C9RA05651C.

[24] Winiarz JG, Zhang L, Lal M, Friend CS, Prasad PN. Photogeneration, charge transport, and photoconductivity of a novel PVK/CdS-nanocrystal polymer composite. Chem Phys. 1999;245(1):417–28. doi: 10.1016/S0301-0104(99)00057-9.

[25] Yao JH, Elder KR, Guo H, Grant M. Theory and simulation of Ostwald ripening. Phys Rev B. 1993;47(21):14110–25. doi: 10.1103/PhysRevB.47.14110.

[26] Qi L, Cölfen H, Antonietti M. Synthesis and characterization of CdS nanoparticles stabilized by double-hydrophilic block copolymers. Nano Lett. 2001;1(2):61–5. doi: 10.1021/nl0055052.

[27] Lee Y-J, Kim T-G, Sung Y-M. Lattice distortion and luminescence of CdSe/ZnSe nanocrystals. Nanotechnology. 2006;17(14):3539–42. doi: 10.1088/0957-4484/17/14/030.

[28] Dutta JDJ. Encyclopedia of nanoscience and nanotechnology. Vol. 4. CA, USA: American Scientific Publishers; 2004.

[29] Murugadoss G, Ramasamy V. Synthesis, effect of capping agents and optical properties of manganese-doped zinc sulphide nanoparticles. Luminescence. 2013;28(1):69–75. doi: 10.1002/bio.2346.

[30] Xaba T, Moloto MJ, Al-Shakban M, Malik MA, Moloto N, O'Brien P. The influences of the concentrations of "green capping agents" as stabilizers and of ammonia as an activator in the synthesis of ZnS nanoparticles and their polymer nanocomposites. Green Process Synth. 2017;6(2):173–82. doi: 10.1515/gps-2016-0089.

[31] Alexandridis P. Gold nanoparticle synthesis, morphology control, and stabilization facilitated by functional polymers. Chem Eng Technol. 2011;34(1):15–28. doi: 10.1002/ceat.201000335.
[32] Ghosh Chaudhuri R, Paria S. Core/shell nanoparticles: classes, properties, synthesis mechanisms, characterization, and applications. Chem Rev. 2012;112(4):2373–433. doi: 10.1021/cr100449n.
[33] Jadhav SA. Functional self-assembled monolayers (SAMs) of organic compounds on gold nanoparticles. J Mater Chem. 2012;22(13):5894–9. doi: 10.1039/C2JM14239B.
[34] Castro JV, Dumas C, Chiou H, Fitzgerald MA, Gilbert RG. Mechanistic information from analysis of molecular weight distributions of starch. Biomacromolecules. 2005;6(4):2248–59. doi: 10.1021/bm0500401.
[35] Torres FG, Troncoso OP, Torres C, Díaz DA, Amaya E. Biodegradability and mechanical properties of starch films from Andean crops. Int J Biol Macromol. 2011;48(4):603–6. doi: 10.1016/j.ijbiomac.2011.01.026.
[36] Martins A, Chung S, Pedro AJ, Sousa RA, Marques AP, Reis RL, et al. Hierarchical starch-based fibrous scaffold for bone tissue engineering applications. J Tissue Eng Regenerat Med. 2009;3(1):37–42. doi: 10.1002/term.132.
[37] Nakamatsu J, Torres FG, Troncoso OP, Min-Lin Y, Boccaccini AR. Processing and characterization of porous structures from chitosan and starch for tissue engineering scaffolds. Biomacromolecules. 2006;7(12):3345–55. doi: 10.1021/bm0605311.
[38] Salgado AJ, Gomes ME, Chou A, Coutinho OP, Reis RL, Hutmacher DW. Preliminary study on the adhesion and proliferation of human osteoblasts on starch-based scaffolds. Mater Sci Eng C. 2002;20(1):27–33. doi: 10.1016/S0928-4931(02)00009-7.
[39] Torres FG, Boccaccini AR, Troncoso OP. Microwave processing of starch-based porous structures for tissue engineering scaffolds. J Appl Polym Sci. 2007;103(2):1332–9. doi: 10.1002/app.25345.
[40] El-Hag Ali A, AlArifi A. Characterization and in vitro evaluation of starch based hydrogels as carriers for colon specific drug delivery systems. Carbohydr Polym. 2009;78(4):725–30. doi: 10.1016/j.carbpol.2009.06.009.
[41] Elvira C, Mano J, San Roman J, Reis R. Starch-based biodegradable hydrogels with potential biomedical applications as drug delivery systems. Biomaterials. 2002;23(9):1955–66.
[42] Malafaya P, Elvira C, Gallardo A, San Roman J, Reis R. Porous starch-based drug delivery systems processed by a microwave route. J Biomater Sci Polym Ed. 2001;12(11):1227–41.
[43] Pereira C, Cunha A, Reis R, Vazquez B, San Roman J. New starch-based thermoplastic hydrogels for use as bone cements or drug-delivery carriers. J Mater Sci Mater Med. 1998;9(12):825–33.
[44] Santander-Ortega M, Stauner T, Loretz B, Ortega-Vinuesa JL, Bastos-González D, Wenz G, et al. Nanoparticles made from novel starch derivatives for transdermal drug delivery. J Controlled Rel. 2010;141(1):85–92.
[45] Ali AE-H, AlArifi A. Characterization and in vitro evaluation of starch based hydrogels as carriers for colon specific drug delivery systems. Carbohydr Polym. 2009;78(4):725–30.
[46] Reis RL, Cunha AM. Characterization of two biodegradable polymers of potential application within the biomaterials field. J Mater Sci Mater Med. 1995;6(12):786–92. doi: 10.1007/BF00134318.
[47] Shahverdi S, Hajimiri M, Esfandiari MA, Larijani B, Atyabi F, Rajabiani A, et al. Fabrication and structure analysis of poly (lactide-co-glycolic acid)/silk fibroin hybrid scaffold for wound dressing applications. Int J Pharm. 2014;473(1):345–55. doi: 10.1016/j.ijpharm.2014.07.021.
[48] Proshchenko V, Dahnovsky Y. Long-lived emission in Mn doped CdS, ZnS, and ZnSe diluted magnetic semiconductor quantum dots. Chem Phys. 2015;461(C):58–62. doi: 10.1016/j.chemphys.2015.09.001.
[49] Verma M, Patidar D, Sharma K, Saxena N. Synthesis, characterization and optical properties of CdSe and ZnSe quantum dots. J Nanoelectron Optoe. 2015;10:320–6. doi: 10.1166/jno.2015.1768.
[50] Gong K, Kelley DF, Kelley AM. Resonance Raman spectroscopy and electron–phonon coupling in zinc selenide quantum dots. J Phys Chem C. 2016;120(51):29533–9. doi: 10.1021/acs.jpcc.6b12202.
[51] Brodu A, Ballottin MV, Buhot J, van Harten EJ, Dupont D, La Porta A, et al. Exciton fine structure and lattice dynamics in InP/ZnSe core/shell quantum dots. ACS Photonics. 2018;5(8):3353–62. doi: 10.1021/acsphotonics.8b00615.
[52] Soheyli E, Sahraei R, Nabiyouni G, Nazari F, Tabaraki R, Ghaemi B. Luminescent, low-toxic and stable gradient-alloyed Fe:ZnSe(S)@ZnSe(S) core:shell quantum dots as a sensitive fluorescent sensor for lead ions. Nanotechnology. 2018;29(44):445602. doi: 10.1088/1361-6528/aada29.
[53] Yang L, Zhu J, Xiao D. Synthesis and characterization of ZnSe:Fe/ZnSe core/shell nanocrystals. J Lumin. 2014;148(C):129–33. doi: 10.1016/j.jlumin.2013.12.013.
[54] Tavakkoli Yaraki M, Tayebi M, Ahmadieh M, Tahriri M, Vashaee D, Tayebi L. Synthesis and optical properties of cysteamine-capped ZnS quantum dots for aflatoxin quantification. J Alloy Compd. 2017;690:749–58. doi: 10.1016/j.jallcom.2016.08.158.
[55] Vidhya K, Saravanan M, Bhoopathi G, Devarajan VP, Subanya S. Structural and optical characterization of pure and starch-capped ZnO quantum dots and their photocatalytic activity. Appl Nanosci. 2015;5(2):235–43. doi: 10.1007/s13204-014-0312-7.
[56] Kuppayee M, Vanathi Nachiyar GK, Ramasamy V. Enhanced photoluminescence properties of ZnS:Cu^{2+} nanoparticles using PMMA and CTAB surfactants. Mat Sci Semicon Proc. 2012;15(2):136–44. doi: 10.1016/j.mssp.2011.09.006.
[57] Qadri SB, Skelton EF, Hsu D, Dinsmore AD, Yang J, Gray HF, et al. Size-induced transition-temperature reduction in nanoparticles of ZnS. Phys Rev B. 1999;60(13):9191–3. doi: 10.1103/PhysRevB.60.9191.
[58] Silverstein RMBG, Morrill TC. Spectrometric identification of organic compounds. John Wiley & Sons. Inc; 1981. https://www.researchgate.net/profile/Wafaa-Hassan-3/publication/306182409_Phytochemical_and_biological_study_of_Albizia_lebbeck_stem_bark/links/5b31161c0f7e9b0df5c7f393/Phytochemical-and-biological-study-of-Albizia-lebbeck-stem-bark.pdf.
[59] Santhiya D, Subramanian S, Natarajan KA, Malghan SG. Surface chemical studies on the competitive adsorption of poly(acrylic acid) and poly(vinyl alcohol) onto alumina.

J Colloid Interface Sci. 1999;216(1):143–53. doi: 10.1006/jcis.1999.6289.
[60] Qiao F, Kang R, Liang Q, Cai Y, Bian J, Hou X. Tunability in the optical and electronic properties of ZnSe microspheres via Ag and Mn doping. ACS Omega. 2019;4(7):12271–7. doi: 10.1021/acsomega.9b01539.
[61] Li C, Zhang H, Cheng C. CdS/CdSe co-sensitized 3D SnO2/TiO2 sea urchin-like nanotube arrays as an efficient photoanode for photoelectrochemical hydrogen generation. RSC Adv. 2016;6(44):37407–11. doi: 10.1039/C6RA02176J.
[62] Lohar GM, Dhaygude HD, Patil RA, Ma Y-R, Fulari VJ. Studies of properties of Fe^{2+} doped ZnSe nano-needles for photoelectrochemical cell application. J Mater Sci Mater Electron. 2015;26:8904–14.
[63] Liu B, Ning L, Zhao H, Zhang C, Yang H, Liu S. Visible-light photocatalysis in Cu2Se nanowires with exposed {111} facets and charge separation between (111) and ( ) polar surfaces. Phys Chem Chem Phys. 2015;17(20):13280–9. doi: 10.1039/C5CP00450K.
[64] Riha SC, Johnson DC, Prieto AL. Cu2Se nanoparticles with tunable electronic properties due to a controlled solid-state phase transition driven by copper oxidation and cationic conduction. J Am Chem Soc. 2011;133(5):1383–90. doi: 10.1021/ja106254h.
[65] Cao M, Wang Y, Guo C, Qi Y, Hu C, Wang E. A simple route towards CuO nanowires and nanorods. J Nanosci Nanotechnol. 2004;4(7):824–8. doi: 10.1166/jnn.2004.822.